Characterization of MoSi Superconducting Single-Photon Detectors in the Magnetic Field

Alexander A. Korneev, Yuliya P. Korneeva, Mikhail Yu. Mikhailov, Yuri P. Pershin, Alexander V. Semenov, D. Yu. Vodolazov, Alexander V. Divochiy, Yuri B. Vakhtomin, Konstantin V. Smirnov, Alexander G. Sivakov, Alexander Yu. Devizenko, and Gregory N. Goltsman

Abstract—We investigate the response mechanism of nanowire superconducting single-photon detectors (SSPDs) made of amorphous Mo_xSi_{1-x}. We study the dependence of photon count and dark count rates on bias current in magnetic fields up to 113 mT at 1.7 K temperature. The observed behavior of photon counts is similar to the one recently observed in NbN SSPDs. Our results show that the detecting mechanism of relatively high-energy photons does not involve the vortex penetration from the edges of the film, and on the contrary, the detecting mechanism of low-energy photons probably involves the vortex penetration from the film edges.

Index Terms—Infrared single-photon detectors, superconducting MoSi films, vortices in superconducting thin films.

I. Introduction

RECENTLY, the physics of superconducting single-photon detectors (SSPDs) has been studied extensively. In particular, the role of vortices in the photon and dark counts was investigated for the SSPDs made of TaN and NbN [1]–[3].

A. A. Korneev and A. V. Semenov are with the Moscow State Pedagogical University, Moscow 119991, Russia, and also with the Moscow Institute of Physics and Technology, Dolgoprudny 141700, Russia (e-mail: akorneev@ rplab.ru).

Y. P. Korneeva is with the Moscow State Pedagogical University, Moscow 119991, Russia.

M. Y. Mikhailov and A. G. Sivakov are with the Institute for Low Temperature Physics and Engineering, National Academy of Sciences of Ukraine, 61103 Kharkiv, Ukraine.

Y. P. Pershin and A. Y. Devizenko are with the National Technical University "Kharkiv Polytechnic Institute," 61000 Kharkiv, Ukraine.

A. V. Divochiy, Y. B. Vakhtomin, and K. V. Smirnov are with CJSC "Superconducting Nanotechnology" (Scontel), Moscow 119435, Russia.

D. Y. Vodolazov is with the Institute for Physics of Microstructures, Russian Academy of Sciences, 603950 Nizhny Novgorod, Russia, and also with Lobachevsky State University of Nizhny Novgorod, 603950 Nizhny Novgorod, Russia.

G. N. Goltsman is with the Moscow State Pedagogical University, Moscow 119991, Russia, and also with the National Research University Higher School of Economics, Moscow 101000, Russia.

Understanding of the vortex mechanism of photon detection in SSPDs opens the way to the improvement of detection efficiency in infrared and reduction of dark counts.

In tantalum nitride (TaN) SSPDs, Engel *et al.* [4] studied the dependence of photon and dark count rates in magnetic fields below 10 mT. It was shown that the origin of dark counts was the vortices crossing according to the prediction of [1]. However, for small energy photons that cannot trigger the detection event directly, no evidence of vortex assistance was observed.

Lusche *et al.* [5] studied the behavior of NbN meanders in the magnetic field. It was shown that both photon and dark counts in NbN meanders are in a good agreement with the vortex model if one uses fitting parameters that are different from the parameters of the theory, based on the "hot" belt model [1]. For the dark count rate, the vortex energy was almost independent of the bias current, whereas for photon counts, it decreased with the bias current, suggesting that photon and dark counts originate from different parts of the meander [5].

Recently, novel promising amorphous materials have been introduced for SSPDs such as WSi and MoSi. These materials are feasible for integration of SSPDs in optical cavities as they are less sensitive to the quality of the substrate compared to crystalline NbN, NbTiN, and others. Marsili *et al.* [6] demonstrated that WSi SSPDs reached a detection efficiency of 93% when cooled down to a 120 mK temperature. Meanwhile, we have recently demonstrated that MoSi SSPDs achieve almost 20% detection efficiency at 1.7 K [7].

In this paper, we study the role of the vortices in the detection mechanism and dark counts of SSPDs made of an amorphous MoSi (a-MoSi) film.

II. Device Fabrication

Our devices are fabricated from a 5.6-nm-thick amorphous $Mo_{0.75}Si_{0.25}$ film as a 105-nm-wide meander strip covering $7~\mu m \times 7~\mu m$ area. The a-Mo_xSi_{1-x} film is deposited on thermally oxidized (100) Si wafers by magnetron co-sputtering from pure Mo and pure Si targets. The thickness of the oxide layer is 250 nm, which allows us to use it as a $\lambda/4$ cavity for 1550-nm photons, similar to the approach proposed in [8]. We do not heat the wafer, and its temperature never goes higher than 100 °C during the deposition process. To prevent a-MoSi film oxidation, we cover it with a 3-nm-thick Si capping layer. During the natural oxidation process, the silicon thickness of this layer reduces to approximately 1.5 nm, and an approximately 2.5-nm-thick SiO_x layer grows on top of it. Due to its
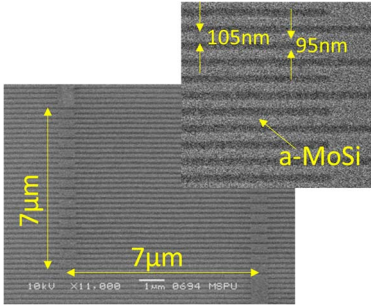
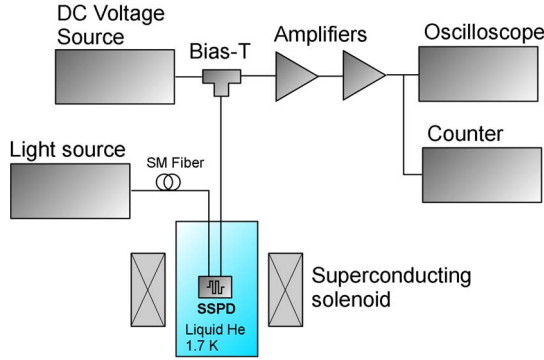Fig. 1.　SEM image of the a-MoSi SSPD. Light gray is the superconducting strip; dark is the etched area.

Fig. 2.　Experimental setup.

low thickness, this capping almost does not affect the optical properties of the detector.

The patterning of the meander is performed by electron-beam (e-beam) lithography in ZEP 520-A7 electron resist and reactive ion etching in SF_6 plasma. Contact pads are made as Cr/Cu bilayers and patterned by photolithography. We believe that due to the large area of the contact pads (about 3 mm^2), the capping layer below them inevitably should have pinholes providing good electrical contact to the a-MoSi layer.

Fig. 1 presents the SEM image of the SSPD used in our experiments. The strip width is 105 nm, and the gap between the strips is 95 nm. The strips surrounding the meander do not carry current, and they are primarily used for proximity effect correction during e-beam lithography. Secondary, they prevent the diffraction at the edges of the meander, thus making simulation of the optical absorption easier.

III. Experimental Setup

Fig. 2 presents the experimental setup that we use for SSPD characterization in the magnetic field. In our experiments, the detectors are cooled down to 1.7 K temperature by helium vapor evacuation from a cryoinsert for a storage dewar. The magnetic field is created by a superconducting solenoid and is applied perpendicularly to the SSPD plane.

The SSPD is dc biased by the precision voltage source through a broadband bias-T. Absorption of a photon produces a voltage pulse that is amplified by two room temperature amplifiers Mini-Circuits ZFL-1000LN+ (1-GHz band, 46-dB total amplification) and fed to a digital oscilloscope and a pulse counter.

The light is delivered to the SSPD by a single-mode optical fiber SMF-28e with a 9-μm mode field diameter. As a light source, we used a grating spectrometer with a black body.

IV. Measurement Results and Discussion

A significant parameter determining detection efficiency in all models of the detection mechanism is a ratio between bias current and depairing current. Depairing current can be calculated within Usadel theory as [9], [10]

$$I_{\mathrm{dep}} = 1.3 \frac{k_B T_c}{e R_s} \frac{w}{\xi_0} f_I \left(\frac{T}{T_c} \right) \quad (1)$$

where R_s is the sheet resistance of the film, and $\xi_0 = (\hbar D / 1.76 k_B T_c)^{1/2}$ is the zero-temperature coherence length. Dimensionless function $f_I(x)$ determines the ratio of the depairing current to that at zero temperature and can be calculated only numerically; the result of such a calculation is presented in [10].

Table I presents material parameters for the studied device: Diffusivity D is determined by the measurement of H_{c2} at different temperatures and will be published elsewhere. Room temperature sheet resistance R_s and resistivity ρ are determined from the sample resistance, film thickness d, and strip width and length. Film thickness d was determined from the film deposition rate and deposition time. Superconducting gap at zero temperature Δ_0 is calculated from T_c using the Bardeen–Cooper–Schrieffer relation $\Delta_0 = 1.76 \ k_B T_c$, where critical temperature T_c is estimated form R versus T curves. Density of states at Fermi level N_0 as well as coherence length $\xi(0)$ and second critical magnetic field H_{c2} at zero temperature are calculated from ρ and diffusivity D, which was extracted from critical temperature versus magnetic field measurements. From these parameters, I_{dep} can be estimated as lying within the range of 40–60 μA (uncertainty is due to pronounced dependence on T_c, which we were not able to measure accurately enough). This indicates that the detector is biased by current that is several times smaller than I_{dep}, similar to SSPDs made of other materials [4], [5].

Dependence of measured critical current I_c on perpendicular magnetic field B at 1.7 K is presented in Fig. 3. The solid line is a theoretical fit made in an assumption that the magnetic field caused redistribution of bias current density across the width of the strip according to

$$I_c(B) = I_c(0) - \frac{w^2}{2 L_s} B \quad (2)$$

where L_s is the kinetic inductance of the film square. Calculating it as

$$L_s = \frac{\hbar R_s}{5.5 \ k_B T_c} f \left(\frac{T}{T_c} \right) \cong 75 \text{ pH} \quad (3)$$

where function $f(T/T_c)$ accounts for the temperature dependence of L_s. For $T/T_c \leq 1/3$ $f(T/T_c) \approx 1$ [10], thus, we obtain the slope of bias current dependence on the magnetic field $I(B)$ as $w^2/2L_s \cong 70 \ \mu$A/T, in agreement with our measurements (see Fig. 3). This supports that action of magnetic field

TABLE I
MATERIAL PARAMETERS OF THE STUDIED DEVICE

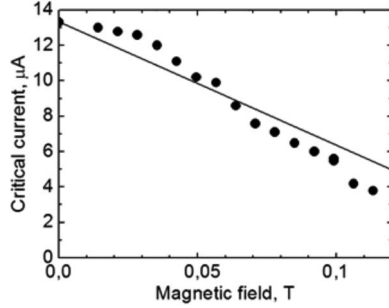| D, m²/s	Rs, Ω (T=300K)	d, nm	ρ, Ω×m	Δ_0, J	Tc, K	N_0, J⁻¹×m⁻³	$\xi(0)$, nm	H_{c2}, T
2.4×10^{-5}	260	5.6	1.46×10^{-6}	1.48×10^{-22}	6	1.0×10^{48}	4	20

Fig. 3. Dependence of the critical current on the applied magnetic field measured at 1.7 K temperature. The solid line is a theoretical fit obtained with the assumption that the magnetic field causes the current redistribution across the strip width.
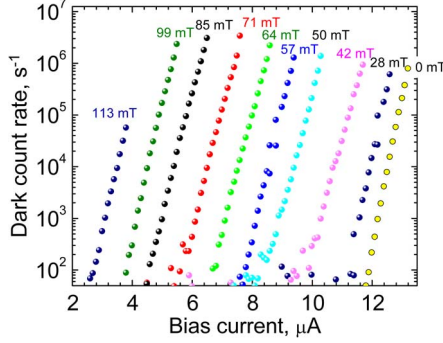

Fig. 4. Dark count rate versus bias current in various magnetic fields ranging from 0 to 113 mT.

on current in our sample adds up to redistribution of current density, as it took place for TaN [4] and NbN [5] samples.

Next, we measured the dark count rate in the magnetic field at 1.7 K. For this measurement, we blocked the input of the fiber. It allowed us to measure the dark count rate R_{dk} in the range $50-5\times10^6$ counts/s. Measurements below 50 counts/s were hampered by the stray light and room temperature background; thus, we excluded them from our analysis. The measured R_{dc} versus bias current in magnetic fields ranging from 0 to 113 mT are presented in Fig. 4. Notice the shift of dependence $R_{dc}(I)$ according to the change in the critical current $I_c(B)$ (compare Figs. 3 and 4) and almost linear dependence of $\log(R_{dc}) \sim I/I_c(B)$ at different magnetic fields, which implies that the dark counts are originating from the vortex crossing the film. Similar effects of the magnetic field on the dark count rate and the critical current of the meander were observed for other materials, such as TaN and NbN [4], [5].

Finally, we measured light counts at wavelengths 450, 600, 800, and 1000 nm in various magnetic fields. The results are shown in Fig. 5. The light counts demonstrate the trend similar to that observed in [5]: 1) detection efficiency increases with increased applied field; 2) the rate of efficiency increase gets faster for lower energy photons; 3) the increase of the detection efficiency is higher for the lower detection efficiency at zero
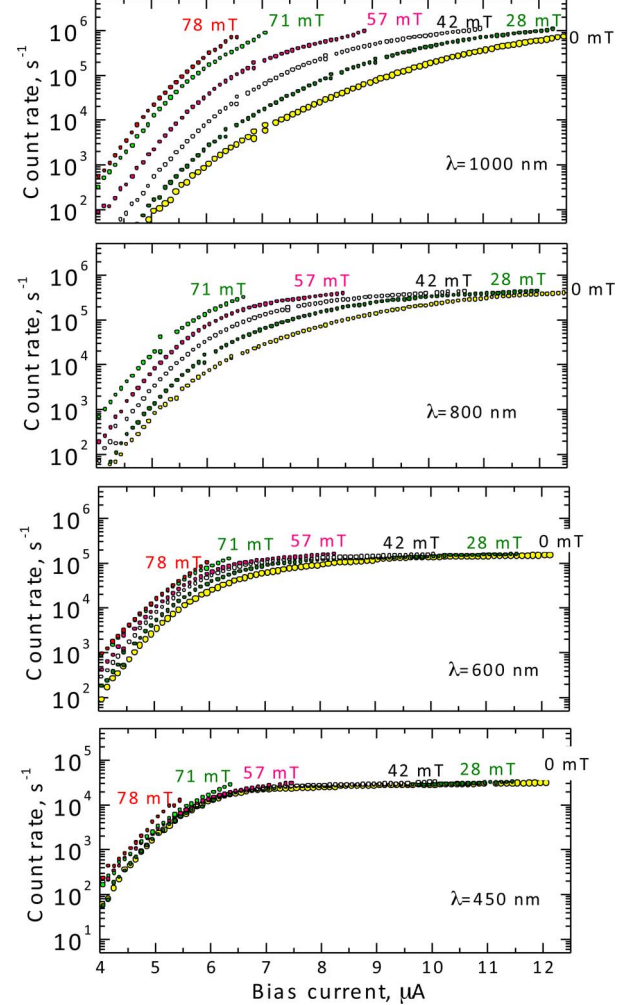

Fig. 5. Photon count rate in different magnetic fields ranging from 0 to 78 mT measured at wavelengths of 450, 600, 800, and 1000 nm. One can observe that with the decrease of photon energy, the contribution of vortices in the detection mechanism increases.

field (at low bias); and 4) at all wavelengths up to 1000 nm, the detection efficiency changes with B significantly slower than the dark count rate.

If one tries to fit the dependence of photon count rate (at fixed current) on the magnetic field $R(B)/R(0)$ using the prediction of the "hot" belt model [1], [5]

$$\frac{R(B)}{R(0)} \approx \cosh\left((v_h + 1)\frac{I_c}{I_b}\frac{B}{B_s}\right) \qquad (4)$$

then one finds the value and dependence $v_h(\lambda)$ that are rather different from the theoretical expectation (similar observation was made in [5]). In (4), B_s is the characteristic field defined as $B_s = 2L_k I_c/w^2 \approx 0.2$ T, and v_h is the fitting parameter that accounts for the suppression of condensation energy in the hot belt due to photon absorption.

Moreover, according to the theory from [1], the threshold current I_{thr}, at which the photon count rate saturates with increasing I, corresponds to the critical current of the film with the hot belt. It means that it should linearly decrease in weak magnetic field as the critical current of the film without the hot belt. Such a behavior is practically absent for the photon with the highest energy ($\lambda = 450$ nm), for which one could expect the best agreement with the hot belt model (notice that the threshold current $I_{\mathrm{thr}} \sim 6 - 7$ μA for this photon is not far below from the critical current $I_c(0) \sim 13$ μA, which would mean that the superconductivity could be not considerably suppressed inside the hot belt).

In the recent modified hot-spot model [11], the weak dependence of the threshold current on the magnetic field was found. This result comes from weak dependence of the critical current of the film with the hot spot, located at the center of the film, on the magnetic field. At such a location, the resistive state starts from nucleation of the vortex–antivortex pair inside the hot spot (and not the vortex entry via the edges of the film), which is the origin of this effect. However, this result poorly explains the effect of magnetic field for low-energy photon ($\lambda = 1000$ nm), when there is noticeable dependence $I_{\mathrm{thr}}(B)$.

To conclude, we characterized MoSi SSPDs via measuring their dark and photo counts in the magnetic field. Our results show that the detection mechanism of relatively high-energy photons most probably does not involve the vortex penetration from the edges of the film, because otherwise, we would observe the dependence of the threshold current on the magnetic field, resembling the dependence $I_c(B)$. Contrary, the detection mechanism of low-energy photons probably involves the vortex penetration from the edges of the film. Our result demonstrates that further development of the existing models of photon detection is needed.

REFERENCES

[1] L. N. Bulaevskii, M. J. Graf, and V. G. Kogan, "Vortex-assisted photon counts and their magnetic field dependence in single-photon superconducting detectors," *Phys. Rev. B, Condens. Matter*, vol. 85, no. 1, Jan. 2012, Art. ID. 014505.

[2] A. N. Zotova and D. Y. Vodolazov, "Photon detection by current-carrying superconducting film: A time-dependent Ginzburg–Landau approach," *Phys. Rev. B, Condens. Matter*, vol. 85, no. 1, Jan. 2012, Art. ID. 024509.

[3] J. J. Renema *et al.*, "Experimental test of theories of the detection mechanism in a nanowire superconducting single photon detector," *Phys. Rev. Lett.*, vol. 112, no. 11, Mar. 2014, Art. ID. 117604.

[4] A. Engel, A. Schilling, K. Il'in, and M. Siegel, "Dependence of count rate on magnetic field in superconducting thin-film TaN single-photon detectors," *Phys. Rev. B, Condens. Matter*, vol. 86, no. 14, Oct. 2012, Art. ID. 140506.

[5] R. Lusche *et al.*, "Effect of magnetic field on the photon detection in thin superconducting meander structures," *Phys. Rev. B, Condens. Matter*, vol. 89, no. 10, Mar. 2014, Art. ID. 104513.

[6] F. Marsili *et al.*, "Detecting single infrared photons with 93% system efficiency," *Nat. Photon.*, vol. 7, no. 3, pp. 210–214, Mar. 2013.

[7] Y. P. Korneeva *et al.*, "Superconducting single-photon detector made of MoSi film," *Supercond. Sci. Technol.*, vol. 27, no. 9, Sep. 2014, Art. ID. 095012.

[8] M. G. Tanner *et al.*, "Enhanced telecom wavelength single-photon detection with NbTiN superconducting nanowires on oxidized silicon," *Appl. Phys. Lett.*, vol. 96, no. 22, May 2010, Art. ID. 221109.

[9] A. Anthore, H. Pothier, and D. Esteve, "Density of states in a superconductor carrying a supercurrent," *Phys. Rev. Lett.*, vol. 90, no. 12, Mar. 2003, Art. ID. 127001.

[10] J. R. Clem and V. G. Kogan, "Kinetic impedance and depairing in thin and narrow superconducting films," *Phys. Rev. B, Condens. Matter*, vol. 86, no. 17, Nov. 2012, Art. ID. 174521.

[11] A. N. Zotova and D. Y. Vodolazov, "Intrinsic detection efficiency of superconducting single photon detector in the modified hot spot model," *Supercond. Sci. Technol.*, vol. 27, no. 12, Dec. 2014, Art. ID. 125001.